AGU PUBLICATIONS

JGR

Journal of Geophysical Research: Biogeosciences

RESEARCH ARTICLE
10.1002/2014JG002851

Key Points:
- Half-hourly soil CH_4 fluxes were measured by a laser-based chamber system
- Environmental responses of CH_4 fluxes were revealed at hourly time resolution
- Summer rainfall under a monsoon climate suppressed CH_4 absorption

Supporting Information:
- Figure S1

Correspondence to:
A. Sakabe,
sakabea@kais.kyoto-u.ac.jp

Citation:
Sakabe, A., Y. Kosugi, K. Takahashi, M. Itoh, A. Kanazawa, N. Makita, and M. Ataka (2015), One year of continuous measurements of soil CH_4 and CO_2 fluxes in a Japanese cypress forest: Temporal and spatial variations associated with Asian monsoon rainfall, *J. Geophys. Res. Biogeosci.*, *120*, 585–599, doi:10.1002/2014JG002851.

Received 4 NOV 2014
Accepted 5 MAR 2015
Accepted article online 11 MAR 2015
Published online 14 April 2015

One year of continuous measurements of soil CH_4 and CO_2 fluxes in a Japanese cypress forest: Temporal and spatial variations associated with Asian monsoon rainfall

Ayaka Sakabe[1], Yoshiko Kosugi[1], Kenshi Takahashi[2], Masayuki Itoh[3], Akito Kanazawa[1,4], Naoki Makita[1,5], and Mioko Ataka[1]

[1]Laboratory of Forest Hydrology, Graduate School of Agriculture, Kyoto University, Kyoto, Japan, [2]Research Institute for Sustainable Humanosphere, Kyoto University, Kyoto, Japan, [3]Center for Southeast Asian Studies, Kyoto University, Kyoto, Japan, [4]Kyoto Prefecture, Kyoto, Japan, [5]Kansai Research Center, Forestry and Forest Products Research Institute, Kyoto, Japan

Abstract We examined the effects of Asian monsoon rainfall on CH_4 absorption of water-unsaturated forest soil. We conducted a 1 year continuous measurement of soil CH_4 and CO_2 fluxes with automated chamber systems in three plots with different soil characteristics and water content to investigate how temporal variations in CH_4 fluxes vary with the soil environment. CH_4 absorption was reduced by the "Baiu" summer rainfall event and peaked during the subsequent hot, dry period. Although CH_4 absorption and CO_2 emission typically increased as soil temperature increased, the temperature dependence of CH_4 varied more than that of CO_2, possibly due to the changing balance of activities between methanotrophs and methanogens occurring over a wide temperature range, which was strongly affected by soil water content. In short time intervals (30 min), the responses of CH_4 and CO_2 fluxes to rainfall were different for each plot. In a dry soil plot with a thick humus layer, both fluxes decreased abruptly at the peak of rainfall intensity. After rainfall, CO_2 emission increased quickly, while CH_4 absorption increased gradually. Release of accumulated CO_2 underground and restriction and recovery of CH_4 and CO_2 exchange between soil and air determined flux responses to rainfall. In a wet soil plot and a dry soil plot with a thinner humus layer, abrupt decreases in CH_4 fluxes were not observed. Consequently, the Asian monsoon rainfall strongly influenced temporal variations in CH_4 fluxes, and the differences in flux responses to environmental factors among plots caused large variability in annual budgets of CH_4 fluxes.

1. Introduction

Methane (CH_4) is an important greenhouse gas, contributing approximately 32% of the radiative forcing of the global climate [*Stocker et al.*, 2013]. The principal sources of CH_4 include fossil fuels, waste decomposition, rice cultivation, domestic ruminants, biomass burning, wetlands, and freshwaters [*Kirschke et al.*, 2013]. On the other hand, the major sink for CH_4 is through chemical reaction with hydroxyl radicals in the troposphere [*Lelieveld and Crutzen*, 1992]. CH_4 consumption in soils due to microbial oxidation by methanotrophs is the only significant biological sink, representing about 1.4–7.4% of the total global sink [*Kirschke et al.*, 2013]. Above all, forest soils are recognized as the most efficient sinks for atmospheric CH_4 [*Le Mer and Roger*, 2001]. The average and standard deviation (SD) of CH_4 fluxes in forest soils around the world were reviewed by *Dutaur and Verchot* [2007], and the highest CH_4 absorption flux and largest variability were observed in temperate forests: 1.13 ± 1.11 nmol m^{-2} s^{-1} in temperate forests (number of sites, $n = 92$), 0.52 ± 0.56 nmol m^{-2} s^{-1} in boreal forests ($n = 51$), and 0.66 ± 0.43 nmol m^{-2} s^{-1} in tropical forests ($n = 62$). Thus, CH_4 fluxes in temperate forests are thought to have larger spatial variability than those in other types of forests. However, the mechanisms mediating these characteristics are not sufficiently clear.

In terms of environmental factors, CH_4 absorption increases as soil water content decreases and as temperature increases [*Steudler et al.*, 1989; *Whalen et al.*, 1990; *Adamsen and King*, 1993; *Dobbie and Smith*, 1996]. Most of these studies have been performed in North America and Europe, where high CH_4 absorption is observed in the summer due to high temperatures and low precipitation [*Dobbie and Smith*, 1996; *Broken and Brumme*, 2000; *Steinkamp et al.*, 2001]. In contrast, CH_4 absorption under climates with humid summers, such as the Asian monsoon climate, is likely to be greatly influenced by intensive summer rainfall. *Morishita et al.* [2007] measured

soil CH_4 fluxes at 26 forest sites in Japan and reported that there are no clear seasonal changes in CH_4 fluxes at most sites. Moreover, they suggested that the efficient promotion of CH_4 absorption by increased temperature may be impeded by the simultaneous increase in soil moisture associated with intensive summer precipitation. Additionally, *Itoh et al*. [2009] measured soil CH_4 fluxes from the upper to lower hillslope areas within Japanese cypress forests. The CH_4 absorption flux significantly differs depending on the sampling location on the hillslope, and changes in soil water content following precipitation were shown to affect CH_4 fluxes in all plots. In particular, summer soil water content affects the estimated annual CH_4 fluxes. In wetter areas, the soil can switch from a CH_4 sink in a dry year to a CH_4 source in a wet year [*Itoh et al*., 2009]. These previous works revealed the comprehensive ranges of CH_4 fluxes throughout Japan and the considerable influence of the Asian monsoon summer rainfall on CH_4 absorption ability.

Most soil CH_4 fluxes have been measured by manually operated chamber methods, with a weekly or monthly time resolution [*Morishita et al*., 2007; *Itoh et al*., 2009]. While manual measurement has its merits, i.e., that multiple measurement points are possible, this method suffers from limited information on relatively short-term variations in fluxes. As for CO_2, several studies using continuous measurements of soil respiration have revealed that CO_2 emission increases immediately (within less than 1 h) after rain events [*Lee et al*., 2004; *Xu et al*., 2004]. These studies demonstrated that continuous measurement is imperative for accurate estimation of soil respiration and net ecosystem production. The same is true of CH_4 fluxes. Moreover, the CH_4 flux is determined by the balance between two conflicting responses: CH_4 production by methanogens and CH_4 oxidation by methanotrophs, which are dependent on soil moisture status (redox conditions) and may therefore change rapidly with rainfall. In the Asian monsoon climate in particular, high precipitation occurs in the summer when CH_4 production increases [*Itoh et al*., 2009]. Considering the substantial effects of rainfall on the variations in CH_4 fluxes, continuous measurement with high time resolution is necessary for making measurements immediately before, during, and after rainfall. CH_4 flux in forest soils is known to show large spatial variation according to topographic conditions [*Ishizuka et al*., 2000; *Morishita et al*., 2007]; however, few studies have investigated how the seasonal variations or responses to rainfall differ according to topographic conditions.

Recently, the development of a laser-based CH_4 analyzer has made it possible to perform in situ continuous measurements of CH_4 concentrations. In this study, we employed this laser-based CH_4 analyzer to measure soil CH_4 and CO_2 fluxes continuously in a Japanese temperate cypress forest by using automated chambers. We examined three characteristic plots in order to investigate how these CH_4 fluxes changed temporally at each plot. Therefore, the aim of this study was to elucidate (i) the ranges of CH_4 fluxes; (ii) the seasonal variations in CH_4 fluxes and environmental factors (soil temperature and soil water content), which influenced their seasonality at each plot; (iii) the detailed temporal responses of CH_4 fluxes to rainfall and how they differed depending on the local topography at each plot; and (iv) the annual budgets of CH_4 fluxes that took into consideration the rainfall responses. While we primarily focused on variations in CH_4 flux, simultaneous measurements in CO_2 flux provided information on the mechanisms controlling the CH_4 flux in the context of microbial activity and gas diffusivity. Moreover, comparing the environmental response of CH_4 fluxes to that of CO_2 fluxes helped us to understand the characteristics of CH_4 fluxes. Our findings are expected to contribute to our understanding of the mechanisms determining soil CH_4 flux in forests under the Asian monsoon climate.

2. Materials and Methods

2.1. Site Description

The observations were made in a temperate coniferous forest in the Kiryu Experimental Watershed (KEW; 35°N, 136°E; 190–255 m above sea level; 5.99 ha), located in Shiga Prefecture, central Japan (Figure 1a). The entire watershed was underlain by weathered granite, with abundant amounts of albite. The soil type was typical brown forest soil and predominantly cambisols. *Ohte et al*. [1997] detailed the physical and chemical properties of the soil in the watershed. The forest consisted of 55 year old Japanese cypress (*Chamaecyparis obtusa* Sieb. et Zucc.), which was planted in 1959. The trees at this site were not disturbed or diseased. The mean tree height was approximately 17.3 m, and the mean diameter at breast height was 0.19 m in 2014. The forest also contained sparsely distributed Japanese red pine (*Pinus densiflora*) and broadleaf trees.

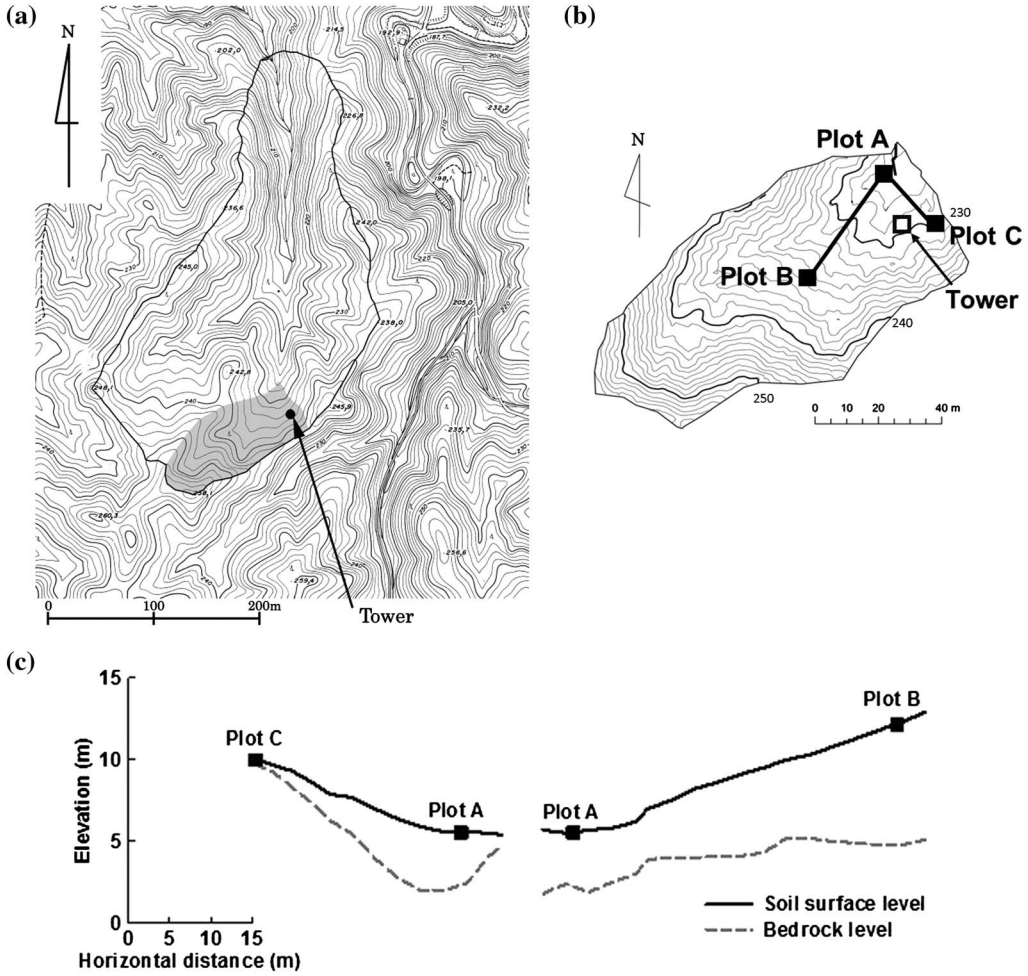

Figure 1. Site description of the Kiryu Experimental Watershed forest in Japan. (a) Topographic large-scale map; gray shading indicates the location of the study site. (b) Topographic small-scale map of the study site. The squares denote the location of three measurement plots and the micrometeorological tower. (c) Longitudinal and cross sections along the lines indicated in Figure 1b. The squares denote the location of measurement plots.

The study site had a warm temperate monsoon climate. The annual mean air temperature and precipitation measured at KEW from 2000 to 2010 were 13.4°C and 1578 mm yr^{-1}, respectively. Rainfall occurred throughout the year with two peaks in the summer due to the Asian monsoon: the early summer "Baiu" front season and the late summer typhoon seasons.

At the study site, canopy fluxes of heat, water, and CO_2 have been measured by the eddy covariance method [*Takanashi et al*., 2005; *Kosugi and Katsuyama*, 2007; *Kosugi et al*., 2007; *Ohkubo et al*., 2007]. Canopy CH_4 flux has also been measured by the relaxed eddy accumulation method [*Sakabe et al*., 2012]. This study revealed how the entire forest ecosystem complexly switched between being a CH_4 source or sink with changes at the hourly, diurnal, and seasonal scales. Soil CH_4 fluxes from wetlands located in riparian zones along streams within KEW and water-unsaturated forest floors were investigated using manually operated chambers with a gas chromatograph analyzer as mentioned above [*Itoh et al*., 2005, 2007, 2009]. Neither CH_4 emission nor absorption from the leaves and trunk was detected by continuous measurement using the automated chamber system [*Takahashi et al*., 2012].

2.2. Sampling Plot

We established three sampling plots within the small catchment (gray shaded zone in Figures 1a and 1b). The catchment had a sloped topography, and the water content in the soils differed depending on the location of the slope. The plots were located in (1) the lower part of the slope adjacent to the stream, with a subsurface

Table 1. Soil Properties in Each Plot at Three Vertical Profiles

	Soil Depth (cm)								
	Plot A			Plot B			Plot C		
Parameter	0–0.05 m	0.05–0.1 m	0.1–0.2 m	0–0.05 m	0.05–0.1 m	0.1–0.2 m	0–0.05 m	0.05–0.1 m	0.1–0.2 m
Porosity (%) $n = 10$	64.4 ± 6.2			63.8 ± 4.3			57.4 ± 4.5		
Bulk density (g cm^{-3}) $n = 10$	0.89 ± 0.19			0.87 ± 0.13			1.03 ± 0.14		
EC(mS m^{-1}) $n = 3$	8.7 ± 6.1	3.6 ± 0.2	3.1 ± 0.5	6 ± 1.5	3.6 ± 0.6	3 ± 0.6	2.9 ± 0.6	2.5 ± 1	1.9 ± 0.7
pH (H_2O) $n = 3$	4.5 ± 0.6	4.8 ± 0.3	4.9 ± 0.1	4.9 ± 0.5	4.9 ± 0.3	5.2 ± 0.6	5.2 ± 0.2	5.3 ± 0.6	5.8 ± 0.6
Total C (mg g^{-1}) $n = 3$	167.5 ± 96.5	20.2 ± 1.4	17.1 ± 6.5	88.4 ± 14.8	20.2 ± 2.6	12.8 ± 3.7	18.4 ± 3.9	15.7 ± 11	5.5 ± 2.1
Total N (mg g^{-1}) $n = 3$	6.9 ± 3.4	1.6 ± 0.1	1.3 ± 0.4	4.4 ± 0.8	1.6 ± 0.2	1.1 ± 0.2	1.4 ± 0.1	1.2 ± 0.5	0.6 ± 0.2
C/N ratio $n = 3$	23.4 ± 3.1	13 ± 0.7	13 ± 0.7	20.1 ± 2.3	12.8 ± 1.1	11.4 ± 1	13.3 ± 2.1	12.3 ± 3.1	8.5 ± 1.6

aquifer year round (plot A); (2) the middle part of the slope, with a subsurface aquifer except during the driest period (plot B); and (3) the upper part of the slope, generally lacking a subsurface aquifer (plot C), as shown in Figures 1b and 1c [*Ohte et al*., 1995]. The maximum distance between plots was approximately 40 m (between plots A and B). In plot A, the top layer of the forest floor consisted of fractional fresh and partly decomposed leaves (0.02–0.03 m depth), below which there was a 0.05 m deep A horizon, these layers were termed the litter layer and humus layer, respectively. The depth from soil surface to the bedrock level was 3.2 m. In plot B, the top layer also consisted of a litter layer (0–0.02 m depth), below which there was a 0.07 m deep humus layer. The depth from the soil surface to the bedrock level was 7.5 m. In plot C, there was a shallow litter layer (0–0.01 m depth) and no humus layer. The depth from the soil surface to the bedrock level was 0.3 m (Table 1).

Mineral and organic soil samples were obtained in bulk at each of the three plots, representing vertical profiles, on 1 May 2013. Topsoil samples (0–0.05, 0.05–0.10, and 0.10–0.20 m) were obtained ($n = 3$ at each depth). Soils were sieved through a 2 mm mesh sieve to remove coarse fragments and then homogenized. Soil pH was determined in a 1:5 w/v air-dried soil/distilled water mixture using a glass electrode pH meter (S40, Mettler Toledo, Switzerland). Electric conductivity (EC) was determined for the same slurry using a conductivity meter (CM-30 V, TOA, Japan). The soil total carbon (C) and nitrogen (N) were measured with a CN analyzer (Sumigraph NC-900, Sumigraph Co., Japan).

2.3. CH_4 and CO_2 Production in Forest Soils During Anaerobic Incubation

We conducted anaerobic incubation of the soils (0–0.03 m depth) for the three sampling plots to investigate CH_4 production potential at each plot. Soil samples were collected on 26 August 2014 under hot and humid conditions, when CH_4 production was supposed to be the most active at any point during the year. Soils were sieved through a 2 mm mesh sieve, and wet soil samples (10 g) were submerged in distilled water to a volume of 10 mL in 65 mL glass vials, which were sealed with butyl rubber stoppers and capped with plastic caps within 6 h after sampling ($n = 10$ at each plot). The soil solutions were purged, and headspace gas was replaced completely with pure N_2 gas using needles that reached the solution. Vials were incubated under static conditions in the dark at 30°C. CH_4 and CO_2 concentrations in the vial headspace were sampled and injected into the gas chromatographs equipped with flame ionization detectors and a thermal-conductivity detector (GC-2014, Shimadzu, Japan) using a gas-tight syringe (injection volume of 0.3 mL for each measurement). Vials were shaken gently before gas concentration measurements. Measurements were carried out 1, 2, 3, 9, and 21 days after starting incubation. We calculated the CH_4 and CO_2 production rates under anaerobic conditions by dividing the amount of produced gases by the incubation period. Potential CH_4 and CO_2 production rates are expressed on a dry soil basis (oven dried at 105°C for 48 h).

2.4. CH_4 Absorption and CO_2 Emission Measurements

Soil surface CH_4 absorption and CO_2 emission were measured using dynamic closed chambers with automatically opening and closing lids (30 cm × 30 cm × 20 cm = L × W × H). A chamber was installed at each plot. The same system was used to measure CH_4 fluxes from the leaves and trunk [*Takahashi et al*., 2012]. The collars were inserted tightly into the ground up to 5 cm in depth prior to the start of the sampling period. A small fan (3 cm × 3 cm × 1 cm) was installed in the chamber to homogenize the inside air. Air from the sample chamber was circulated to a CO_2/H_2O analyzer (LI-840; Li-Cor Inc., Lincoln, NE, USA) and a laser-based spectrometer CH_4

analyzer (FMA-200; Los Gatos Research, Mountain View, CA, USA) through polyethylene tubes (inner tube: 4 mm in diameter) by a diaphragm pump (APN-085, IWAKI PUMPS, Tokyo, Japan; DM-403ST-25, MFG. CO., LTD., Kyoto, Japan) controlled using a mass flow controller (MPC0005, Yamatake, Tokyo, Japan) at a flow rate of 1.8 L min^{-1}. After measuring, the sampled air was returned to the chamber. Opening and closing of the chamber lid were controlled by pressurized air supplied by an air compressor (FH-02, MEIJI, Osaka, Japan). The switching among the chambers was regulated by the solenoid valves (CKD USB3-6-3-E, CKD Corp., Aichi, Japan) and a 16 channel alternating current/direct current controller (SDM-CD16AC, Campbell Scientific, UT, USA). Three filters were inserted in the gas sample line to protect the CH_4 analyzer from dust and insects. Before entering the CO_2/H_2O and CH_4 analyzers, the sampled air was dried using a gas dryer (PD-50 T-48, Perma Pure Inc., Toms River, NJ, USA). Dilution by water vapor, which could not be completely removed by the drying system, was corrected using the H_2O concentration measured with the CO_2/H_2O analyzer.

Chamber measurements were repeated every 30 min. Data were recorded at 1 Hz using a CR1000 data logger (CR1000, Campbell Scientific) and stored on a compact flash card using a compact flash module (CFM100, Campbell Scientific). A 2 s moving average filtered the high-frequency noises for the CO_2/H_2O analyzer, and a 1 s moving average was used for the CH_4 analyzer. The data analyzed in this study were recorded from 1 August 2009 to 31 August 2010. Data were missing from 19 to 24 September 2009 in plot B, from 9 to 24 September 2009 in plot C due to chamber instrumental malfunctions, and from 29 June to 6 August 2010 in all plots due to CH_4 analyzer malfunctions.

CH_4 and CO_2 fluxes were deduced from the rate of change of gas concentrations with time, as determined using linear regression as follows (equation (1)).

$$\text{flux} = \frac{dc}{dt} \times \frac{V}{S} \times \rho_{\text{amol}} \tag{1}$$

where $\frac{dc}{dt}$ is the rate of increase in the gas concentration c (ppm) with time t (s); $\frac{dc}{dt}$ is determined from the slope of the change in gas concentration from 90 to 170 s from the start of measurement using the linear least squares method; V is the volume of the chamber (0.018 m^3); S is the surface area of the chamber (0.09 m^2); and ρ_{amol} is the air mole density (mol m^{-3}). Generally, negative flux means net CH_4 absorption, whereas positive flux does net CH_4 emission. In this paper, however, we present positive flux values as CH_4 absorption in order to simplify the comparison between CH_4 and CO_2 flux variations. The zero offset of the CO_2/H_2O and CH_4 analyzers was checked against nitrogen gas every day at 12:15 h. The CO_2/H_2O analyzer was calibrated every few months using a standard CO_2 gas cylinder and a humidity calibrator (HG-1, Michell Instruments, Tokyo, Japan). To examine the accuracy and precision of our CH_4 analyzer, calibration experiments were performed on site using a standard CH_4 gas cylinder (Takachiho, Tokyo, Japan; 1773 ppb CH_4 in synthetic air) during the course of this study. The performance of the CH_4 analyzer was tested using the Allan variance method [e.g., *Eugster and Plüss*, 2010]. This assessment suggested that the Allan deviation of our analyzer was 0.7 ppb, with a 1 s integration time at atmospheric levels of CH_4 [*Takahashi et al.*, 2012]. The possible error in CH_4 flux, estimated from the overall precision of our system at atmospheric levels of CH_4, was 0.5 nmol m^{-2} s^{-1}.

2.5. Environmental Monitoring

Volumetric soil water content (VWC) at a depth of 0–30 cm was measured with a CS616 water content reflectometer (Campbell Scientific) at each plot. Soil moisture was converted into water-filled pore space (WFPS) as follows: WFPS = VWC/total pore volume. Total pore volume was measured in the laboratory with ten 100 mL undisturbed soil samples taken from a mineral soil layer at each plot. Soil temperatures were measured with copper-constantan thermocouples at depths of 2 cm just adjacent to each of the three chambers. Precipitation was measured with a tipping bucket rain gauge at an open screen site near the tower.

2.6. Gap Filling

To evaluate the annual budgets of CH_4 absorption and CO_2 emission fluxes, we applied the linear interpolation method for gaps within 6 h and the mean diurnal variation (MDV) method [*Falge et al.*, 2001] for gaps longer than 6 h. The MDV was created for each day with a 15 day moving window. CH_4 and CO_2 fluxes were filled 19.2% and 18.8% in plot A, 19.2% and 18.7% in plot B, and 20.1% and 19.6% in plot C.

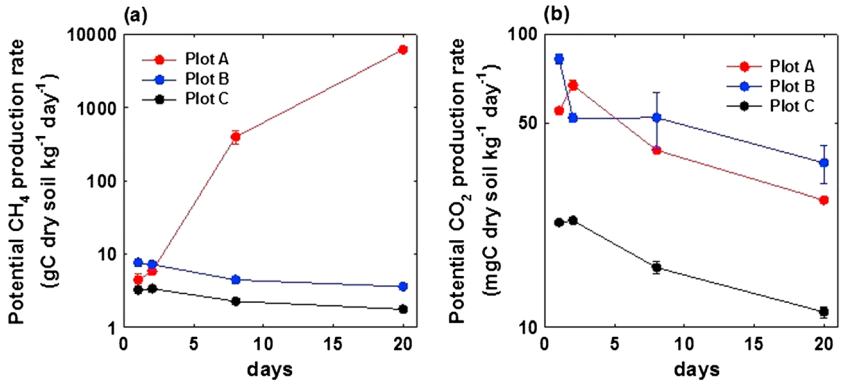

Figure 2. The potential production rates of (a) CH_4 and (b) CO_2 of sampled soils in each plot 1, 2, 8, and 20 days after the first measurement day. The samples were incubated at 30°C. Means and standard deviations (error bars) are shown ($n = 10$).

2.7. Statistical Analysis

The mean and SD of CH_4 absorption and CO_2 emission over the entire measurement period in each plot were calculated using half-hourly fluxes. Mean fluxes are presented as the mean ± SD. The ranges of CH_4 absorption and CO_2 emission were calculated from half-hourly fluxes. One-way analysis of variance with post hoc Games-Howell test at the 0.05 significance level was used to compare the means of topsoil C and N concentrations and potential CH_4 and CO_2 production rates at each plot. This analysis was performed with SPSS (Statistical Package for the Social Science) Statistics 21 (IBM SPSS Statistics, IBM Corp., Armonk, NY, USA).

3. Results

3.1. Soil Properties

There were no significant differences in the topsoil (0–0.05 m) pH and EC among plots (Table 1). The topsoil N concentration ranged from 6.9 mg g^{-1} (plot A) to 1.4 mg g^{-1} (plot C). The topsoil C concentration ranged from 167.5 mg g^{-1} (plot A) to 13.4 mg g^{-1} (plot C). The topsoil N and C concentrations in plot C were significantly lower than those in plot A ($p < 0.05$ and $p = 0.041$, respectively). This is probably because sandy soil with larger particle sizes was more common in plot C. Plot B had moderate N and C concentrations among the three plots, i.e., lower than plot A and higher than plot C; however, these differences were not significant. The topsoil C/N ratio ranged from 23.4 (plot A) to 13.5 (plot C). The C/N ratio in plot C was significantly lower than those of plots A and B ($p < 0.01$ and $p < 0.05$, respectively). There were no significant differences in topsoil C/N ratios between plots A and B.

3.2. CH_4 and CO_2 Production in Forest Soils During Anaerobic Incubation

In terms of the potential to produce CH_4, no CH_4 production was observed the next day after incubation at all plots, except for one soil in plot A (Figure 2a). Two days after incubation, CH_4 production was observed at all plots. Nine days after incubation, a sharp increase in CH_4 production was observed in plot A, and this distinguished plot A from the other two plots. In plot C, both potential CH_4 and CO_2 production rates were significantly lower than those in the other plot throughout the experimental period ($p < 0.01$; Figures 2a and 2b).

3.3. Time Course Analysis of Soil Environment, CH_4 Absorption, and CO_2 Emission

Figure 3 illustrates annual variations in daily average soil temperature, precipitation, and WFPS and 30 min CH_4 absorption and CO_2 emission fluxes in each plot. Higher soil temperatures and more precipitation were observed in summer than in winter (Figure 3a). Among plots, plot A had higher WFPS than plots B and C throughout the experimental period (Figure 3b). Although plot C also had higher WFPS than plot B, the WFPSs in plots B and C were smaller than those of plot A for all seasons. The CH_4 absorption fluxes ranged from −0.45 to 1.25 nmol m^{-2} s^{-1} (annual average, 0.38 ± 0.16 nmol m^{-2} s^{-1}) in plot A, from 0.13 to 3.70 nmol m^{-2} s^{-1} (annual average, 2.16 ± 0.49 nmol m^{-2} s^{-1}) in plot B, and from −1.20 to 2.02 nmol m^{-2} s^{-1} (annual average, 0.44 ± 0.34 nmol m^{-2} s^{-1}) in plot C (Figure 3c). The CO_2 emission fluxes ranged from 0.22 to 6.17 μmol m^{-2} s^{-1} (annual average, 2.44 ± 1.46 μmol m^{-2} s^{-1}) in plot A, from 0.26 to 7.55 μmol m^{-2} s^{-1} (annual average,

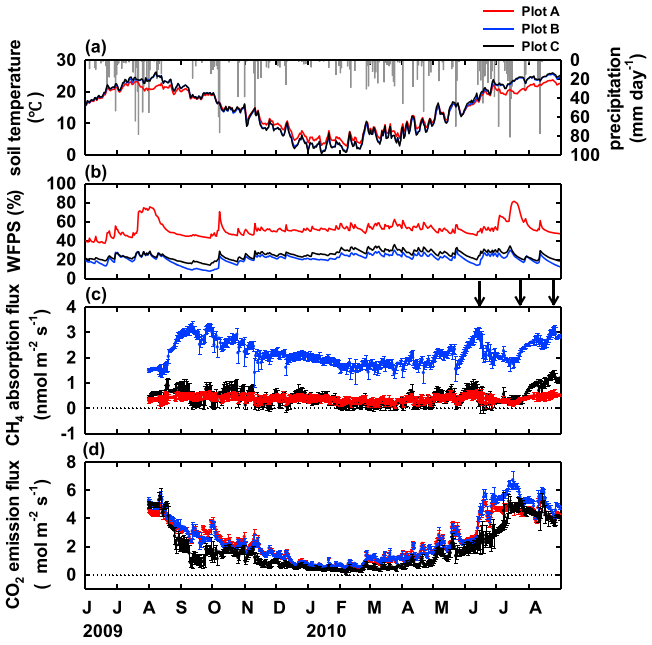

Figure 3. Annual variations in daily averaged (a) soil temperature and precipitation, (b) WFPS, (c) 30 min CH_4 absorption, and (d) 30 min CO_2 emission in each plot from 1 August 2009 to 31 August 2010.

$2.57 \pm 1.73\ \mu mol\ m^{-2}\ s^{-1}$) in plot B, and from -0.94 to $7.13\ \mu mol\ m^{-2}\ s^{-1}$ (annual average, $1.81 \pm 1.54\ \mu mol\ m^{-2}\ s^{-1}$) in plot C (Figure 3d).

Annual budgets of CH_4 absorption from 1 September 2009 to 31 August 2010 were $142\ mg\ C\ m^{-2}\ yr^{-1}$ in plot A, $825\ mg\ C\ m^{-2}\ yr^{-1}$ in plot B, and $162\ mg\ C\ m^{-2}\ yr^{-1}$ in plot C (Table 2). Those of CO_2 emission were $871\ mg\ C\ m^{-2}\ yr^{-1}$ in plot A, $912\ mg\ C\ m^{-2}\ yr^{-1}$ in plot B, and $608\ mg\ C\ m^{-2}\ yr^{-1}$ in plot C. In plot A, which was characterized by thick organic layers and a high WFPS, the annual budget of CH_4 absorption was the smallest among plots; however, the annual budget of CO_2 emission was the second largest after plot B. In plot B, which was characterized by a thick humus layer and a low WFPS, the annual budgets of CH_4 absorption and CO_2 emission were the highest among plots. In plot C, which was characterized by a thin humus layer and a low WFPS, the annual budgets of CH_4 absorption and CO_2 emission were significantly smaller than those in plot B. The coefficients of variation for both CH_4 and CO_2 fluxes in plot C were the highest among plots.

3.4. Effects of Soil Temperature and Moisture on Seasonal Variations in CH_4 Absorption

CH_4 absorption showed seasonal variations in every plot (Figure 3c), and the largest variation was observed in plot B. Although the ranges of CH_4 absorption fluxes in plots A and C were smaller than that in plot B, a similar seasonal pattern of CH_4 absorption was observed in every plot. The rainy season Baiu occurred in June 2009, and the Baiu front became active in late July 2009. In addition, the typhoon "Etau" brought much rain from 8 August to 11 August 2009 (32.8 mm within 96 h). After heavy rainfall, CH_4 absorption became small in early August 2009 and gradually increased as WFPS decreased from late August 2009. The highest absorption among plots in 2009 was observed on 29 September in plot B. In early October 2009, the typhoon "Melor" brought much rain (136.2 mm within 48 h), and CH_4 absorption decreased. A gradual decrease was observed as the temperature decreased. The WFPS was maintained at relatively high levels during the winter, and there was no remarkable decline in CH_4 absorption. In plot B, CH_4 absorption increased again as the temperature increased in spring 2010. However, CH_4 absorption was decreased by the summer intensive rainfall, and Baiu began on 13 June 2010 (shown as the first arrow in Figure 3c). From 17 July, after the Baiu, CH_4 absorption increased again as WFPS decreased and temperature increased (shown as the second arrow in Figure 3c). The highest absorption in 2010 was observed on 26 August in plot B when the soil temperature was high and the soil was dried (shown as the third arrow in Figure 3c). The seasonal variation in soil CH_4 absorption was strongly influenced by intensive summer rainfall resulting from the Asian monsoon climate and typhoon at our site. In contrast, the seasonality in CO_2 emission was strongly correlated with soil temperature in every plot (Figure 3d). High CO_2 emission was observed during summer but decreased as the temperature decreased heading into

Table 2. Annual Budgets of CH_4 Absorption and CO_2 Emission at Each Plot From 1 September 2009 to 31 August 2010

	Plot A	Plot B	Plot C
Annual budget of CH_4 absorption flux ($mg\ C\ m^{-2}\ yr^{-1}$)	142	825	162
Annual budget of CO_2 emission flux ($mg\ C\ m^{-2}\ yr^{-1}$)	871	912	608

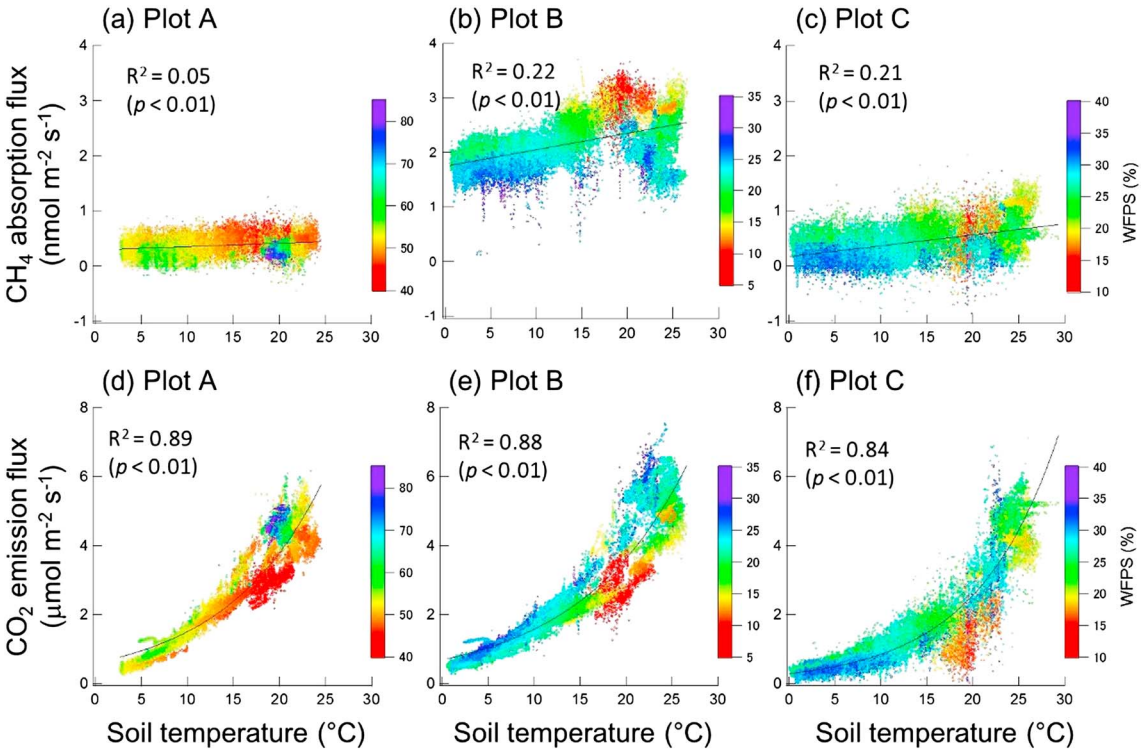

Figure 4. Relationships between soil temperature and CH_4 absorption in (a) plot A, (b) plot B, and (c) plot C. The plots are color-coded according to WFPS. Relationships between soil temperature and CO_2 emission in (d) plot A, (e) plot B (e), and plot C (f). The black line shows the linear equation for CH_4 flux and the first-order exponential equation for CO_2 flux. The determination coefficient R^2 represents the goodness of the fit of the regression model. The probability values of each regression model are shown.

winter. The WFPS also affected the seasonality of CO_2 emission. CO_2 emission decreased when the soil was dried, even at high temperatures, in the middle of September 2009, in late June 2010, and in early August 2010.

We focused on soil temperature and WFPS as major factors controlling the seasonal variations in CH_4 absorption and CO_2 emission. The relationships between soil temperature and CH_4 absorption or CO_2 emission are shown in Figure 4. Linear regression equations for CH_4 fluxes [*Potter et al.*, 1996; *Ridgwell et al.*, 1999; *Del Grosso et al.*, 2000] and first-order exponential equations for CO_2 fluxes [*Lloyd and Taylor*, 1994] were used to determine the coefficient R^2, which measures the goodness of fit of the regression model. All regression models were significant ($p < 0.01$). Both CH_4 absorption and CO_2 emission generally increased as the soil temperature increased in every plot, but CH_4 absorption exhibited larger variation than CO_2 emission. The R^2 of CH_4 fluxes was lower than that of CO_2 fluxes. In particular, the R^2 of the CH_4 flux in plot A was the lowest among plots (Figure 4a). The relationships between soil temperature and CH_4 absorption or CO_2 emission were affected by the WFPS; high WFPS inhibited CH_4 absorption and CO_2 emission in every plot (Figures 4a–4f). CO_2 emissions showed similar temperature dependence among plots, while CH_4 absorption showed unique temperature dependences among plots and was not universal across plots. In plot A, CH_4 absorption increased slightly as soil temperature increased (Figure 4a). In plot B, CH_4 absorption clearly increased from 10°C to 20°C, and the maximum absorption was observed when the soil temperature was 20.3°C and the WFPS was 11.6% (Figure 4b). On the other hand, CH_4 absorption did not increase simply according to the increase in temperature, and a greater variation was observed above 20°C, where CH_4 absorption with high WFPS was low. In plot C, CH_4 absorption increased with increasing temperature above 10°C and had a larger variation at higher temperatures (Figure 4c). The maximum absorption was observed when the soil temperature was 26.2°C and the WFPS was 21.3%.

Figure 5 shows the relationships between WFPS and CH_4 absorption or CO_2 emission flux. Comparing the relationship between WFPS and CH_4 absorption or CO_2 emission, CH_4 absorption was decreased as the WFPS increased at every plot (Figure 5a), while CO_2 emission exhibited varying behaviors upon changes in the

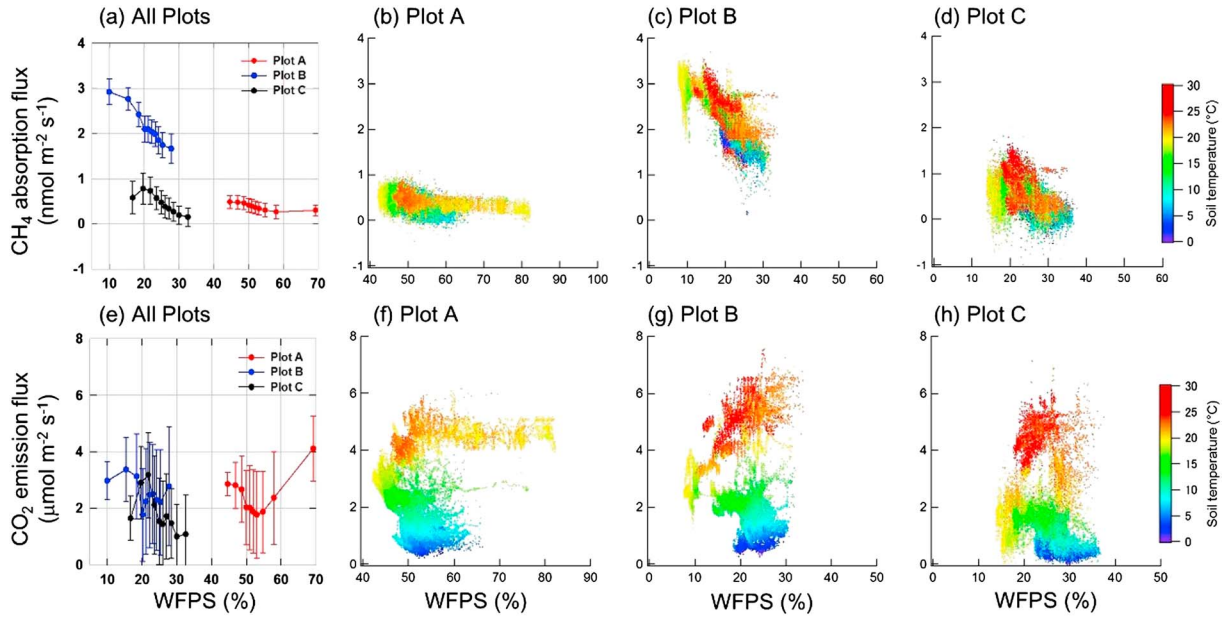

Figure 5. Relationship between WFPS and CH_4 absorption or CO_2 emission in each plot. Half-hourly CH_4 absorption fluxes were binned into 10 classes according to WFPS (a). Circles and error bars represent the average and standard deviation of CH_4 absorption. Relationships between WFPS and CH_4 absorption are color coded according to soil temperatures in (b) plot A, (c) plot B, and (d) plot C. (e) The relationships between WFPS and CO_2 emission were binned into 10 classes according to WFPS, and the relationships were color coded according to soil temperature in (f) plot A, (g) plot B, and (h) plot C.

WFPS (Figure 5e). CH_4 absorption increased as the WFPS decreased over the whole temperature range studied in this work (Figures 5b–5d), while CO_2 emission depended moderately on the WFPS only at high soil temperatures above about 20°C in plots B and C (Figures 5g and 5h). It should also be noted that the relationship between CH_4 absorption and WFPS was not universal but rather unique to each plot (Figure 5a). Additionally, this relationship seemed to be mitigated at the driest conditions. CH_4 absorption seemed to be decreased in plots B and C when the WFPS was relatively low (<20%; Figure 5a). Corresponding CO_2 emissions also seemed to be decreased when the WFPS was relatively low in plots B and C (Figure 5e).

3.5. Responses of CH_4 Absorption and CO_2 Emission to Rainfall

Next, we examined data describing dramatic temporal changes in CH_4 absorption and CO_2 emission due to rainfall. We focused on the responses of CH_4 absorption and CO_2 emission to different total amounts of precipitation at 30 min intervals. Figure 6 shows two representative examples of the plot-dependent responses in CH_4 absorption and CO_2 emission to different rainfall patterns: total rainfall of 38.7 mm with a maximum intensity of 18.1 mm h^{-1} (Figures 6a–6d), and total rainfall of 71.2 mm with a maximum intensity of 10.2 mm h^{-1} (Figures 6e–6h). In both rainfall events, the characteristics of the responses of CH_4 and CO_2 fluxes to rainfall events were similar, but their patterns were different for each plot. These data can be summarized as follows: (1) the most prominent responses among the plots were observed in plot B for CH_4 fluxes; (2) in plot A, remarkable changes in CO_2 flux were observed, while changes in CH_4 flux were not significant; and (3) in plot C, both CH_4 and CO_2 fluxes showed decreases during and after rainfall events.

When we took a closer look at the characteristics of each plot, in plot B, which had a thick humus layer and a normally low WFPS, CO_2 emission increased at the beginning of rainfall in both rainfall events and then decreased abruptly with minima at the peaks of rainfall intensity (Figures 6c and 6g). CH_4 absorption also showed minima at the same time. The reduction in CH_4 absorption and CO_2 emission at the peaks of rainfall intensity were greater in the case of the 71.2 mm rainfall event than the 38.7 mm rainfall event. After rainfall, however, the responses of CH_4 and CO_2 fluxes were different: CO_2 emission showed abrupt increases followed by long decreases, while CH_4 absorption showed only increases. In plot A, which had a thick humus layer and constantly high WFPS, CO_2 fluxes increased at the beginning in both rainfall events (Figures 6b and 6f), similar to those in plot B, but showed maxima at the peak of rainfall intensity. After rainfall, CO_2 fluxes showed long decreases, similar to those in plot B. On the other hand, CH_4 fluxes in plot A

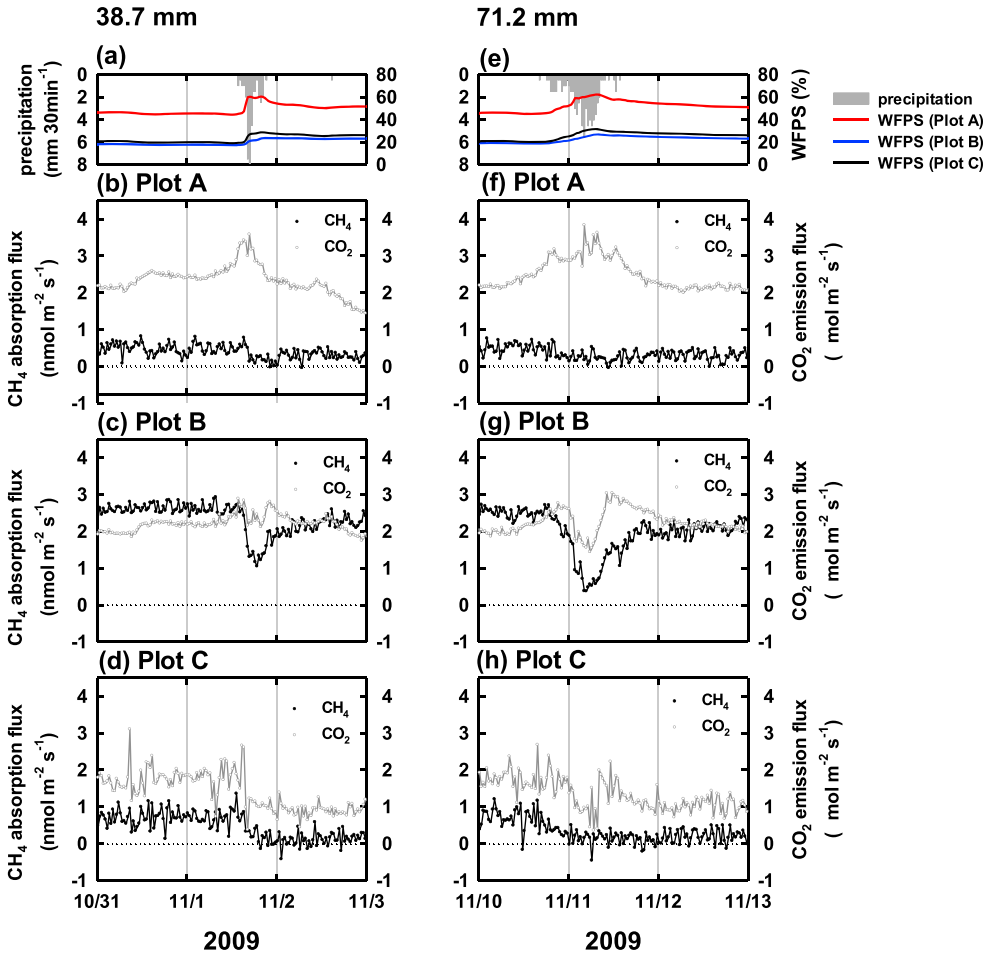

Figure 6. Variations in half-hourly precipitation, WFPS, CH_4 absorption, and CO_2 emission during and after rainfall. (a) Responses in CH_4 absorption and CO_2 emission to 38.7 mm precipitation from 1 November 2009 in (b) plot A, (c) plot B, and (d) plot C, and (e) response to 71.2 mm precipitation from 10 November 2009 in (f) plot A, (g) plot B, and (h) plot C are shown.

did not exhibit dramatic changes with respect to the rainfall events. In plot C, which exhibited a thin humus layer and a low WFPS, both CO_2 and CH_4 fluxes decreased clearly during rainfall events (Figures 6d and 6h). However, in the case of the 71.2 mm rainfall event, CO_2 flux showed a distinct minimum at the peak of the rainfall intensity (Figure 6h). After rainfall, CH_4 fluxes increased quite slowly compared to those in plot B.

Interestingly, in plots A and C, where CH_4 absorption was originally low compared to that in plot B, water-unsaturated forest soil switched from acting as a sink to neutral following rainfall (Figures 6b, 6d, 6f, and 6h). Soil in plot C returned to its role as a CH_4 sink after rainfall, concurrent with the decrease in WFPS.

4. Discussion

4.1. Variations in CH_4 Absorption

In this study, we compared CH_4 absorption among soils with different characteristics in a Japanese temperate Cypress forest. There are three possible reasons for the low-CH_4 absorption in the plot with a thick organic layer and a high WFPS (plot A). First, CH_4 production in wet reductive microsites would have obscured CH_4 oxidation. Even if the surface of the forest floor was usually not saturated with water, CH_4 production could occur deeper within the ground because the area always had a subsurface aquifer. From the incubation experiment, we found that the potential to produce CH_4 was markedly higher in plot A than in the other two plots (Figure 2a). *Itoh et al.* [2009] reported that CH_4 emission occurred during rainy summers from the water-unsaturated forest floor, adjacent to the riparian zone. Moreover, they suggested that their results

weredue to CH_4 production in wet reductive microsites on the lower hillslope and near water pathways [*Itoh et al*., 2005, 2009]. To support this, an increase in the CH_4 gas concentration below the soil surface was observed with increasing soil temperature [*Itoh et al*., 2009]. The balance of CH_4 oxidation and production determines the CH_4 absorption flux; thus, net CH_4 oxidation could be reduced by an increase in CH_4 production in a plot with a high WFPS. We assumed that the surface soil water content and the presence of a subsurface aquifer could affect CH_4 fluxes. Second, higher WFPSs lead to smaller pore space, which may restrict the variation range of the WFPS, causing the variation range of CH_4 absorption in plot A to be smaller than that in the other plots (Figure 3c). Finally, in addition to the anaerobic environment, rich organic matter would contribute to the low CH_4 absorption. Plot A had high C and N concentrations and a high C/N ratio. The high C/N ratio in plot A, which may have resulted from the lower decomposition rate in anaerobic soil than that in aerobic soil, may indicate a reductive environment. A positive correlation between CH_4 production and organic matter content was observed only in the reductive environment, consistent with the observation that organic C is first used by the other reducers before being used by methanogenic bacteria in soils containing significant quantities of oxidants [*Wang et al*., 1993]. Therefore, in plot A, rich organic matter content might activate CH_4 production under a reductive environment. Additionally, CH_4 production is generally thought to be influenced by both the quality and quantity of organic matter present; *Whiting and Chanton* [1993] suggested that recent plant residues or fresh plant materials are the main substrates for methanogens. If the high C and N concentrations in plot A are indicative of increased input from fresh litters, these contents may be usable for methanogens. Although the CH_4 absorption in plot C was also low, the low WFPS would contribute to more pore space and larger variations in the WFPS, which would lead to greater variability in CH_4 absorption than that in plot A.

Interestingly, under low WFPS conditions, the CH_4 absorption flux was significantly higher in plot B, which had a thick humus layer, than in plot C, which had a thin humus layer. In the plot with a thick humus layer and high CO_2 emission (plot B), the rich organic content would supply nutrients for microbes, leading to high CH_4 absorption flux. *Del Grosso et al*. [2000] showed clear contrasts between deciduous forests and other types of ecosystems: the CH_4 oxidation rate in the deciduous forest soils showed a more variable response to soil water content, and this response was generally higher than those observed in other soils. This was thought to be because the high gas diffusivity would promote availability to CH_4 and O_2 for methanotrophs in the porous rich organic layer. In plot C, which had a thin humus layer and lower CO_2 emission than plot B, the low C and N concentrations may lead to low-microbial activity, including that of methanotrophs. We found that the potential to produce CH_4 and CO_2 was the lowest in plot C among the plots examined in our study, although this result was found in the incubation experiment under anoxic conditions. These data suggested that the microbial activity under oxic conditions in plot C was also lower than those in the other two plots.

4.2. Seasonal Variations in Soil CH_4 Absorption, CO_2 Emission, and Environmental Factors

Intensive summer rainfall due to the Asian monsoon climate controlled seasonal variations in soil CH_4 absorption at our study site (Figure 3c). Similarly, *Morishita et al*. [2007] reported that VWC is an important factor mediating seasonal variations in CH_4 fluxes in Japanese forests, and increased CH_4 absorption resulting from increasing temperature is suppressed by intensive summer rainfall. In addition to this earlier study, we found that CH_4 absorption was decreased after an intensive summer rainfall to the level observed in winter and subsequently recovered along with the recovery of the WFPS from continuous measurements. In winter, high CH_4 absorption was not observed because the temperature was low and the WFPS did not decline very much due to low evapotranspiration.

CO_2 emission flux usually has a unidirectional response to temperature: emission increases with increasing temperature. On the other hand, CH_4 absorption should have bidirectional responses to temperature because most methanogens and methanotrophs are mesophiles; thus, both CH_4 consumption and production increase as the temperature increases. *Dunfield et al*. [1993] have shown that methane production and consumption in temperate and subarctic peats are optimum around 20–30°C for both activities, while some researchers have reported that methanotrophy is preferred over methanogenesis at lower temperatures [*King and Adamsen*, 1992; *Castro et al*., 1993; *Sitaula et al*., 2000]. Using incubation experiments using soil cores from a mixed hardwood-coniferous forest, *King and Adamsen* [1992] found that increases in the CH_4 oxidation rate with increasing temperatures occurred only at the lower temperature variation (near 0°C), whereas temperature

increases in the upper range had little effect on CH_4 consumption. Observations in temperate forests showed that methanotrophy was affected between −5 and 10°C but not between 10 and 20°C [*Castro et al*., 1993]. Significant methanotrophy was still observed in forest soils at average temperatures lower than 1°C [*Sitaula et al*., 2000]. At our study site, CH_4 fluxes showed large variability at higher temperatures (Figures 4b and 4c), probably because temperature-dependent increases in the activity of methanotrophs decreased, while methanogens can be active at high temperatures and therefore conceal the activity of methanotrophs. In addition, CH_4 absorption showed a clear dependence on the WFPS throughout the entire temperature range (Figures 5b–5d), while CO_2 flux showed no clear dependence on the WFPS at low temperatures (Figures 5f–5h). This result strongly suggested that the activity of methanogens and/or methanotrophs occurred even at low temperatures. Thus, abiotic factors, such as gas diffusivity, which is controlled by the WFPS, would be also important for CH_4 absorption and/or emission by affecting the exchange of CH_4 and O_2 (as substrates for methanotrophs or inhibitors for methanogens) between soil and air. Moreover, if the location of the source of CH_4 was deep in the soil, the temperature would not change very much compared to that at the surface. Thus, we can assume that, as a result of these factors, the CH_4 absorption flux would show much more complex dependence on temperature than the CO_2 emission flux (Figures 4a–4c). The variability observed in the relationship between the CH_4 absorption flux and soil temperature at high temperatures could be ascribed to the large variability in the WFPS. In summer, the WFPS exhibited greater variability, and the high temperature promoted the activity of methanogens and methanotrophs, resulting in substantial variability in CH_4 flux. In contrast, in winter, the WFPS exhibited smaller variations, and the activity of methanogens and methanotrophs was low due to the low temperature. Therefore, the variability in CH_4 absorption would be small. During the relatively dry period (WFPS $<$ 20%), CH_4 absorption was decreased, even at temperatures as high as 20°C (plots B and C; Figures 5c and 5d). This is because of the decrease in CH_4 absorption resulting from light rainfall (less than 4 mm h^{-1}) during summer with no antecedent rainfall. At this time, our soil water reflectometer (CS616, Campbell) did not respond to light rainfall, but CH_4 absorption was decreased by rainfall in plots B and C. The small variation in soil water content would cause large variations in CH_4 absorption when the soil dried antecedently; thus, such artifact mitigation of CH_4 absorption in the driest period could be observed (see supplementary information).

4.3. Responses of CH_4 Absorption and CO_2 Emission to Rainfall

In general, rainfall caused decreases in CH_4 absorption in every plot, though the extent of the depression was plot dependent. In the plot with a normally low WFPS and thick humus layer (plot B), CH_4 absorption and CO_2 emission showed distinct depressions at the same time at the peak of rainfall intensity (Figures 6c and 6g). The depressions were greater in the case of the 71.2 mm rainfall event than in the case of the 38.7 mm rainfall event. This suggested that the depressions were caused mainly by restricted gas diffusivity at the soil surface by rain water, which would be more restricted as the total amount of rainfall increased. In the plot with a normally high WFPS and thick humus layer (plot A) and the plot with a normally low WFPS and thinner humus layer (plot C), the abrupt depressions in CH_4 fluxes could not be observed clearly, probably because CH_4 absorption was originally low in these plots.

With respect to the differences in responses of CH_4 absorption and CO_2 emission just after rainfall in plot B, CO_2 emission showed abrupt increases followed by long decreases, while CH_4 absorption showed only gradual increases. Such abrupt increases in CO_2 emission could be explained by the observation that accumulated CO_2 in the soil during rainfall would be released immediately after rainfall because of increased gas diffusivity. On the other hand, the restricted gas diffusivity at the soil surface would decrease CH_4 consumption by methanotrophs due to the limited supply of substrate, such as CH_4 and O_2, from the atmosphere [*Steudler et al*., 1989; *Whalen et al*., 1990; *Adamsen and King*, 1993; *Castro et al*., 1993; *MacDonald et al*., 1996; *MacDonald et al*., 1997]. Moreover, CH_4 absorption may be obscured in anoxic soil with increased WFPS due to the decreased activity of methanotrophs and increased activity of methanogens long after rainfall. From the incubation experiment, we found that CH_4 production was observed as early as the next day after starting the incubation (Figure 2a). Therefore, when rainfall occurs intermittently, it is possible that changes in the activities of methanogens and methanotrophs occur soon after rainfall. Another interesting aspect is that the recovery of CH_4 absorption and CO_2 emission after rainfall in plot B was faster than that in plot C. This is probably because the microbial activities, such as those involved in CH_4 consumption and/or CO_2 production, were lower in plot C than in plot B, as suggested from the incubation experiment.

Moreover, in plots A and C, CH_4 absorption shifted from a sink to a neutral state after rainfall. This small, transient shift may be missed under less frequent and less sensitive sampling strategies. Moreover, if the plot exhibiting switching from sink to neutral is large, the effects on canopy-scale fluxes may need to be considered during scale up. Therefore, it is important to understand the process of sink-to-neutral switching (and vice versa) at the plot scale. We showed that CH_4 absorption was greatly decreased by rainfall and subsequently recovered through the process of sink-to-source switching (and vice versa) at the plot scale. Thus, it is possible that the annual budget of CH_4 absorption flux would be overestimated without considering the rain pulse or underestimated without considering the recovery. Consistent with this hypothesis, simulated annual budgets of CH_4 absorption under the assumption that CH_4 fluxes were measured weekly during fair weather (previously no rain for 24 h) and daytime hours (from 09:00 to 15:00 h) were overestimated from 2.8% to 7.6% in plot A, from 0.9% to 5.6% in plot B, and from 3.1% to 20.1% in plot C. Overestimation was significant in plot C, where CH_4 absorption substantially shifted to neutral after rainfall.

As for CO_2 fluxes, CO_2 emission increased in plots A and B, which both had thick humus layers, at the beginning of rainfall (Figures 6b, 6c, 6f, and 6g), while in the plot C, which had a thin humus layer, the CO_2 emission did not increase at the beginning of rainfall (Figures 6d and 6h). This difference may be associated with the high- and low-microbial activities that produce CO_2 [*Orchard and Cook*, 1983]. The higher CO_2 emission in plots A and B than in plot C was consistent with the incubation experiments, despite being measured under anoxic conditions (Figure 2b).

Finally, we note that this type of high time resolution analysis examining the effects of rainfall on CH_4 and CO_2 fluxes was not easily achieved without an automated chamber system coupled to an in situ trace gas analyzer. In particular, we believe that our approach was a powerful and efficient method to study the short time dynamics of CH_4 absorption/emission at the soil surface as well as long-term variations in CH_4 flux.

4.4. Annual Budgets of CH_4 Absorption

We obtained annual budgets of CH_4 absorption by taking into consideration the rainfall responses and compared annual budgets of CH_4 absorption to published data from forest soils around the world, particularly for Japan. The annual budgets of CH_4 absorption in plots A, B, and C were 142, 825, and 162 mg C m^{-2} yr^{-1}, respectively. *Dutaur and Verchot* [2007] reported that the mean annual budgets of CH_4 absorption in boreal, temperate, and tropical forest soils were 198 ± 925 (number of study sites, $n = 51$), 426 ± 249 ($n = 92$), and 249 ± 419 ($n = 62$) mg C m^{-2} yr^{-1}, respectively. Japanese forest soil has been mainly divided into two types: approximately 70% of Japanese forest soils are brown forest soil, mostly cambisols and some andisols, and 13% are black soil (andisols) [*Morisada et al.*, 2004]. Based on the synthesis of soil CH_4 absorption measured at 26 sites, the annual budget of CH_4 absorption fluxes is estimated to be 526 mg C m^{-2} yr^{-1} in brown forest soil and 832 mg C m^{-2} yr^{-1} in black forest soil [*Morishita et al.*, 2007]. Moreover, CH_4 absorption in black soil has been reported to be significantly higher than that in brown soils because the lower bulk density and higher soil porosity of brown soils lead to increasing supply of CH_4 from the atmosphere through soil pores [*Morishita et al.*, 2007]. Within KEW, where the climate is temperate and the soil type is brown forest soil, the annual budget of CH_4 absorption had larger variations than the global average of temperate forests. Moreover, the variation in the annual budget of CH_4 absorption in the plot with a low WFPS and a thick humus layer was comparable to that black forest soil. On the other hand, those in plots with either a high WFPS and thick organic layer or a low WFPS and thin humus layer were smaller than that of brown forest soil, as reported by *Morishita et al.* [2007]. Most modeling to estimate global soil sink for atmospheric CH_4 has focused on the climatic zone, ecosystem type, and soil type. However, the capacity of CH_4 absorption cannot be evaluated by only these factors, and it is necessary to consider spatial variability depending on local soil environments, such as soil water content and the amount of organic matter, temporal variations caused by rainfall, and the observation that the temporal variations greatly differ for the local soil environment.

5. Conclusion

In this study, we conducted continuous and high time resolution measurements of soil CH_4 absorption and CO_2 emission in a Japanese cypress forest in the Asian monsoon climate with intensive summer rainfall using an automated chamber system with a laser-based CH_4 analyzer. We found that the highest CH_4 absorption was observed within the summer; however, the CH_4 absorption was greatly decreased by summer

intensive rainfall and recovered after rainfall as soil water content decreased. The relationship between CH_4 absorption and soil temperature varied more than that of CO_2 within each plot because CH_4 absorption was strongly affected by soil water content and active over a wide temperature range. Notably, the relationships between CH_4 absorption and soil temperature or soil water content were not universal among plots, with differences in soil physical conditions that controlled the gas exchange between the soil and air. In plots with a high WFPS and thick organic layer, CH_4 absorption was low. When comparing CH_4 absorption in two plots with low WFPSs, we found that CH_4 absorption was significantly higher in the plot with a thick humus layer and lower in the plot with a thin humus layer. Moreover, CH_4 absorption was high in the plot in which decomposition would be active and low in the plots in which decomposition would not be active. Importantly, CH_4 absorption was dramatically inhibited during rainfall and recovered after rainfall, and the responses to rainfall were unique to the specific local environment, which influences gas diffusivity and the balance of activity between methanotrophs and methanogens. The response also changed depending on the amount of rainfall. Therefore, when evaluating the expected CH_4 absorption flux in forests, considering these responses of CH_4 fluxes to rainfall is important, especially in the Asian monsoon climate. Simultaneous measurements of CO_2 fluxes will provide useful information when considering the controlling factors affecting complex CH_4 fluxes.

Acknowledgments

The data for this paper are available by contacting the corresponding author. The authors thank M. Tani of Kyoto University for constructive suggestions on this study. This work was supported by the Japanese Ministry of Education, Culture, Sports, Science, and Technology Grant-in-Aid for Scientific Research (21380095 and 23248023) and Grant-in-Aid for Japan Society for the Promotion of Science fellows (12J04356) and in part by a Grant of Frontier Researches in Sustainable Humanosphere, RISH, Kyoto University.

References

Adamsen, A. P. S., and G. M. King (1993), Methane consumption in temperate and subarctic forest soils: Rates, vertical zonation, and responses to water and nitrogen, *Appl. Environ. Microbiol.*, *59*, 485–490.

Broken, W., and R. Brumme (2000), Effects of prolonged soil drought on CH_4 oxidation in a temperate spruce forest, *J. Geophys. Res.*, *105*, 7079–7088, doi:10.1029/1999JD901170.

Castro, M. S., P. A. Steudler, J. M. Melillo, J. D. Aber, and S. Millham (1993), Exchange of N_2O and CH_4 between the atmosphere and soils in spruce-fir forests in the northeastern United States, *Biogeochemistry*, *18*, 119–135.

Del Grosso, S. J., et al. (2000), General CH_4 oxidation model and comparisons of CH_4 oxidation in natural and managed systems, *Global Biochem. Cycles*, *14*, 999–1019.

Dobbie, K. E., and K. A. Smith (1996), Comparison of CH_4 oxidation rates in woodland, arable and set aside soils, *Soil Biol. Biochem.*, *28*, 1357–1365.

Dunfield, P. F., E. Topp, C. Archambault, and R. Knowles (1993), Effect of nitrogen fertilizers and moisture content on CH_4 and N_2O fluxes in a humisol: Measurements in the field and intact soil cores, *Biogeochemistry*, *29*, 199–222.

Dutaur, L., and L. V. Verchot (2007), A global inventory of the soil CH_4 sink, *Global Biogeochem. Cycles*, *21*, GB4013, doi:10.1029/2006GB002734.

Eugster, W., and P. Plüss (2010), A fault-tolerant eddy covariance system for measuring CH_4 fluxes, *Agric. For. Meteorol.*, *150*, 841–851.

Falge, E., et al. (2001), Gap filling strategies for defensible annual sums of net ecosystem exchange, *Agric. For. Meteorol.*, *107*, 43–69.

Ishizuka, S., T. Sakata, and K. Ishizuka (2000), Methane oxidation in Japanese forest soils, *Soil Biol. Biochem.*, *32*, 767–777.

Itoh, M., N. Ohte, M. Katsuyama, K. Koba, M. Kawasaki, and M. Tani (2005), Temporal and spatial variability of methane flux in a temperate forest watershed, *J. Jpn Soc. Hydrol. Water Resour.*, *18*, 244–256.

Itoh, M., N. Ohte, K. Koba, M. Katsuyama, K. Hayamizu, and M. Tani (2007), Hydrologic effects on methane dynamics in riparian wetlands in a temperate forest catchment, *J. Geophys. Res.*, *112*, G01019, doi:10.1029/2006JG000240.

Itoh, M., N. Ohte, and K. Koba (2009), Methane flux characteristics in forest soils under an East Asian monsoon climate, *Soil Biol. Biochem.*, *41*, 388–395, doi:10.1016/j.soilbio.2008.12.003.

King, G. M., and A. P. S. Adamsen (1992), Effects of temperature on methane consumption in a forest soil and in pure cultures of the methanotroph methylomonas rubra, *Appl. Environ. Microbiol.*, *58*, 2758–2763.

Kirschke, S., et al. (2013), Three decades of global methane sources and sinks, *Nat. Geosci.*, *6*, 813–823, doi:10.1038/NGEO1955.

Kosugi, Y., and M. Katsuyama (2007), Evapotranspiration over a Japanese cypress forest: II. Comparison of the eddy covariance and water budget methods, *J. Hydrol.*, *334*, 305–311, doi:10.1016/j.jhydrol.2006.05.025.

Kosugi, Y., S. Takanashi, H. Tanaka, S. Ohkubo, M. Tani, M. Yano, and T. Katayama (2007), Evapotranspiration over a Japanese cypress forest. I. Eddy covariance fluxes and surface conductance characteristics for 3 years, *J. Hydrol.*, *337*, 269–283, doi:10.1016/j.jhydrol.2007.01.039.

Le Mer, J., and P. Roger (2001), Production, oxidation, emission and consumption of methane by soils: A review, *Eur. J. Soil Biol.*, *37*, 25–50.

Lee, X., H. Wu, J. Sigler, C. Oishi, and T. Siccama (2004), Rapid and transient response of soil respiration to rain, *Global Change Biol.*, *10*, 1017–1026, doi:10.1111/j.1365-2486.2004.00787.x.

Lelieveld, J., and P. J. Crutzen (1992), Indirect chemical effects of methane on climate warming, *Nature*, *335*, 339–342.

Lloyd, J., and J. A. Taylor (1994), On the temperature dependence of soil respiration, *Funct. Ecol.*, *8*, 315–323.

MacDonald, J. A., U. Skiba, L. J. Sheppard, E. J. Hargreaves, K. A. Smith, and D. Fowler (1996), Soil environmental variables affecting the flux of methane from a range of forest, moorland and agricultural soils, *Biogeochemistry*, *34*, 113–132.

MacDonald, J. A., U. Skiba, L. J. Sheppard, B. Ball, J. D. Roberts, K. A. Smith, and D. Fowler (1997), The effect of nitrogen deposition and seasonal variability on methane oxidation and nitrous oxide emission rates in an upland spruce plantation and moorland, *Atmos. Environ.*, *31*, 3693–3706.

Morisada, K., K. Ono, and H. Kanomata (2004), Organic carbon stock in forest soils in Japan, *Geoderma*, *119*, 21–32, doi:10.1016/S0016-7061(03)00220-9.

Morishita, T., R. Hatano, O. Nagata, K. Sakai, T. Koide, and O. Nakahara (2007), Effect of nitrogen deposition on CH4 uptake in forest soils in Hokkaido, Japan, *Soil Sci. Plant Nutr.*, *50*, 1187–1194.

Ohkubo, S., Y. Kosugi, S. Takanashi, T. Mitani, and M. Tani (2007), Comparison of the eddy covariance and automated closed chamber methods for evaluating nocturnal CO_2 exchange in a Japanese cypress forest, *Agric. For. Meteorol.*, *142*, 50–65, doi:10.1016/j.agrformet.2006.11.004.

Ohte, N., N. Tokuchi, and M. Suzuki (1995), Biogeochemical influences on the determination of water chemistry in a temperate forest basin: Factors determining the pH value, *Water Resour. Res.*, *31*, 2823–2834, doi:10.1029/95WR02041.

Ohte, N., N. Tokuchi, and M. Suzuki (1997), An in situ lysimeter experiment on soil moisture influence on inorganic nitrogen discharge from forest soil, *J. Hydrol.*, *195*, 78–98.

Orchard, V. A., and F. J. Cook (1983), Relationship between soil respiration and soil moisture, *Soil Biol. Biochem.*, *15*, 447–453.

Potter, C. S., E. A. Davidson, and L. V. Verchot (1996), Estimation of global biogeochemical controls and seasonality in soil methane consumption, *Chemosphere*, *32*, 2219–2246.

Ridgwell, A., S. J. Marshall, and K. Gregson (1999), Consumption of atmospheric methane by soils: A process-based model, *Global Biogeochem. Cycles*, *13*, 59–70, doi:10.1029/1998GB900004.

Sakabe, A., K. Hamotani, Y. Kosugi, M. Ueyama, K. Takahashi, A. Kanazawa, and M. Itoh (2012), Measurement of methane flux over an evergreen coniferous forest canopy using a relaxed eddy accumulation system with tunable diode laser spectroscopy detection, *Theor. Appl. Climatol.*, *109*, 39–49, doi:10.1007/s00704-011-0564-z.

Situala, B. K., S. Hansen, J. I. B. Situala, and L. R. Bakken (2000), Methane oxidation potentials and fluxes in agricultural soil: Effects of fertilization and soil compaction, *Biogeochemistry*, *48*, 323–339.

Steinkamp, R., K. Butterbach-Bahl, and H. Papen (2001), Methane oxidation by soils of an N limited and N fertilized spruce forest in the Black Forest, Germany, *Soil Biol. Biochem.*, *33*, 145–153, doi:10.1016/S0038-0717(00)00124-3.

Steudler, P. A., R. D. Bowden, J. M. Melillo, and J. D. Aber (1989), Influence of nitrogen fertilization on methane uptake in temperate forest soils, *Nature*, *341*, 314–316.

Stocker, T. F., et al. (2013), Technical Summary, in *Climate Change 2013: The Physical Science Basis. Contribution of Working Group I to the Fifth Assessment Report of the Intergovernmental Panel on Climate Change*, edited by T. F. Stocker et al., pp. 659–740, Cambridge Univ. Press, Cambridge, U. K., and New York.

Takahashi, K., Y. Kosugi, A. Kanazawa, and A. Sakabe (2012), Automated closed-chamber measurements of methane fluxes from intact leaves and trunk of Japanese cypress, *Atmos. Environ.*, *51*, 329–332, doi:10.1016/j.atmosenv.2012.01.033.

Takanashi, S., Y. Kosugi, Y. Tanaka, M. Yano, T. Katayama, H. Tanaka, and M. Tani (2005), CO_2 exchange in a temperate Japanese cypress forest compared with that in a cool-temperate deciduous broad-leaved forest, *Ecol. Res.*, *20*, 313–324, doi:10.1017/s11284-005-0047-8.

Wang, Z. P., C. W. Lindau, R. D. Delaune, and W. H. Patrick Jr. (1993), Methane emission and entrapment in flooded rice soils as affected by soil properties, *Biol. Fertil. Soils*, *16*, 163–168.

Whalen, S. C., W. S. Reeburgh, and K. A. Sandbeck (1990), Rapid methane oxidation in a landfill cover soil, *Appl. Environ. Microbiol.*, *56*, 3405–3411.

Whiting, G. J., and J. P. Chanton (1993), Primary production control of methane emission from wetlands, *Nature*, *364*, 794–795.

Xu, L., D. D. Baldocchi, and J. Tang (2004), How soil moisture, rain pulses, and growth alter the response of ecosystem respiration to temperature, *Global Biochem. Cycles.*, *18*, GB4002, doi:10.1029/2004GB002281.